Experimental Mechanics (2007) 47: 143–151
DOI 10.1007/s11340-006-9394-9

SI-Traceable Spring Constant Calibration of Microfabricated Cantilevers for Small Force Measurement

G.A. Shaw · J. Kramar · J. Pratt

Received: 23 November 2005 / Accepted: 5 June 2006 / Published online: 14 September 2006

Abstract A variety of methods exist to measure the stiffness of microfabricated cantilever beams such as those used as mechanical sensors in atomic force microscopy (AFM). In order for AFM to be used as a quantitative small force measurement tool, these methods must be validated within the International System of Units (SI). To this end, two different contact techniques were used to calibrate the spring constant of a cantilever beam. First, a dynamic indentation-based method was used to measure the spring constant of a rectangular cantilever beam. These results were then compared against an SI-traceable spring constant measurement from an electrostatic force balance (EFB). The measurements agree within experimental uncertainty and within 2% for spring constants greater than 2 N/m. The use of this cantilever beam as a transfer artifact for in situ AFM cantilever calibration was then evaluated in comparison to the thermal calibration method. Excellent agreement is seen between these techniques, establishing the consistency of the thermal and dynamic indentation methods with SI-traceable contact cantilever calibration for the rectangular cantilever geometry tested.

G. A. Shaw (✉, SEM member) · J. Kramar · J. Pratt
U.S. National Institute of Standards and Technology,
Manufacturing Engineering Laboratory,
100 Bureau Dr., Gaithersburg, MD 20899, USA
e-mail: gordon.shaw@nist.gov

Keywords Atomic force microscopy · Nanotechnology · Calibration · Mechanical engineering

Introduction

The atomic force microscope (AFM) is unique among the techniques available for localized physical and chemical properties measurements in that it combines dimensional and small force measurement capabilities. Central to these capabilities is the mechanical sensor that interacts directly with the surface being examined. This sensor is typically a microfabricated cantilever that is approximated as a linear spring. The tip of the beam deflects in direct proportion to an applied force following Hooke's law: $F = kz$, where F is applied force, z is the resulting displacement, and k is the spring constant of the system. The use of AFM for dimensional metrology has been established [1]. AFM is primarily used as a tool for imaging surfaces, and is increasingly used for small force measurement. AFM studies exploiting the instrument's force measurement capability have been conducted to examine structural transformations in single DNA [2] and protein molecules [3], to measure the mechanical properties of thin films [4], and even to detect the spin of single electrons [5]. However, the use of AFM for quantitative force metrology is limited by the ability to accurately determine k.

The nominal spring constants provided by cantilever manufacturers are subject to dramatic variation between different lots, or even within the same wafer, so independent methods must be utilized to ensure accuracy in small force measurement. There are a variety of methods available for determining the spring constants of microfabricated cantilevers, each with their

own merits and drawbacks. They are typically grouped into four broad categories: dimensional methods, intrinsic methods, dynamic methods, and static methods.

Dimensional methods involve measuring the dimensions of the cantilever, and using an analytical approximation to determine k. For rectangular cantilevers, Euler–Bernoulli beam theory can be used, giving

$$k = \frac{3EI}{L^3} \tag{1}$$

where E is Young's modulus of the cantilever material, L is cantilever length and I is the moment of inertia for a particular cantilever shape of uniform cross-section. For example, $I = wt^3/12$ is the equation describing the moment of inertia for a rectangular cantilever beam where w, and t are its width and thickness. Beams with a trapezoidal cross-section may also be analyzed by dimensional means [6]. Often, V-shaped cantilevers are used as well, and solutions for the dimensional determination of k have been developed based on a parallel beam approximation [7]. Generally, the accuracy of dimensional methods is limited by uncertainties in measurement of the beam thickness, and in knowledge of the beam material's elastic properties (i.e., Young's modulus). These are compounded when a coating is applied to the cantilever as is often done to enhance reflectivity.

Intrinsic methods rely on natural phenomena that provide a well-defined reference force. Measuring the cantilever deflection in response to this intrinsic force provides a measure of k. The B-S transition of DNA is a change in molecular conformation that appears when the molecule is put into tension, and seems to occur at a force of approximately 65 pN [2]. Single molecule tensile testing studies of the B-S transition are being used as an ad-hoc standard for 65 pN forces in AFM experiments, for example [8].

Dynamic methods rely on measurement of cantilever vibration. In the Cleveland method, the change in resonance frequency of a cantilever is measured as tungsten microspheres of different mass are attached to the cantilever tip [9]. Because the microspheres are challenging to manipulate, this approach is difficult to implement. It also renders the tip unsuitable for imaging, as the sphere must typically be attached to the cantilever with an adhesive. The Sader method relies on measurement of the beam width and length, as well as the resonance frequency and quality factor of the cantilever's first mode of vibration in combination with a viscous damping model to determine a value for k [10]. This procedure can be used with cantilevers of any shape, but relies on experimental determination of viscous damping behavior. The thermal method uses the equipartition theorem to determine cantilever spring constants [11]. If the power spectrum of the thermal vibrations of the cantilever can be measured, an approximate value for k can be determined using this technique. Although it is the easiest of the methods to implement, there are uncertainties arising from the laser spot size, and its location along the cantilever beam [12].

Static methods employ direct measurements of the force necessary to deflect the tip of the cantilever a certain distance at low frequency. They share the disadvantage that the location of the applied force must be specified very precisely since the value of k scales cubically with the distance from the cantilever base to the point of force application as in equation (1). However, these are the most direct methods for determining k, as the force and displacement at the tip of the cantilever are explicitly measured. This provides a means to use with Hooke's law to define a spring constant within the SI, provided the force and displacement can be measured in an SI-traceable manner and their related uncertainties quantified. For this reason, static calibration methods will now be explored in more depth.

At this time, most of the static methods involve a physical contact between the cantilever and another object which is capable of applying a measurable small force. It may be argued that the presence of a physical contact during calibration is most appropriate for cantilevers which will use a physical contact to measure force during final use. However, accurate quantitative measurement of k may be achieved through accurate measurement of non-contact forces, such as those generated by magnetic, electrostatic or gravitational fields. A non-contact cantilever calibration has been carried out using gravitational forces from small deadweights. This has been accomplished by attaching a precisely located microsphere of tungsten to an AFM cantilever, and observing the resultant deflection of the tip [13]. Due to their size, the spheres cannot be directly compared to the kilogram, restricting their use in SI-traceable metrology. Instead, mass must be estimated using the bulk density of tungsten, and measurements of the sphere diameter. Measurement of the sphere placement and sphere diameter both limit the accuracy of this technique, as they require painstaking scanning electron microscopy (SEM) dimensional metrology to achieve percent level uncertainties [14].

A different static method for spring constant calibration is to bring an auxiliary force measurement transducer into contact with the cantilever, and apply known forces or displacements between them. Either a passive or an active transducer can be used. Typically, the

passive transducer is an auxiliary cantilever with a known spring constant. If a test cantilever is pressed against a reference cantilever, measuring the deflection signal of the test cantilever allows the determination of its k [15, 16]. Generally, the cantilever under test is displaced in a direction normal to the surface of the reference cantilever, and its deflection is monitored with the optical lever configuration typical of AFM. The piezoelectric actuators in the AFM can be used to displace the cantilever if care is taken to account for the effects of piezo nonlinearity and creep, or to make an independent displacement measurement. Naturally, there is uncertainty associated with the stiffness of the reference cantilever, which must be calibrated itself. This can be minimized for the case of cantilevers that can be mass loaded with deadweights; however SI-traceability below 5 μN of force is difficult through this means since the smallest mass artifact available from a national measurement institute (NMI) is 0.5 mg. SI-traceable electrical forces may present a good alternative to mass loading, though, and work is proceeding in this area [20, 23, 27].

Another static approach to spring constant calibration is to use an active sensor that provides force and/or displacement information. To measure force, a deadweight-calibrated miniature capacitive force sensor can be placed in contact with the AFM cantilever [17]. The use of a commercial indentation apparatus for this purpose is also possible [18, 25, 26, 28]. These indentation instruments have also been used to measure SI-traceable forces to the μN level based on a deadweight calibration of an auxiliary sensor [19], and the ability to apply small SI-traceable forces to calibrate cantilever force sensors using an electrostatic force balance has been demonstrated [20]. As will be shown later, a similar approach can be used to effectively calibrate cantilever stiffness. Dynamic indentation and traceable electrostatic force methods will be explored further in the experimental section, as they provide SI-traceable force and displacement information simultaneously, providing the shortest path for spring constant measurement within the SI.

Materials and Methods

Reference Cantilever

The cantilever under test was the cantilever microfabricated array of reference springs (CMARS) [15]. Designed specifically for the purpose of spring constant calibration, it was fabricated from polycrystalline silicon and is approximately 1,600-μm long, 150-μm wide and 3-μm thick. There are lithographically-defined fiducial marks along the cantilever's length that can be used to locate a specific point for testing. Since the spring constant of a cantilever scales with length^{-3} [cf. equation (1)], this allowed for a wide range of spring constants to be tested.

Dynamic Indentation Method

The spring constant was calculated assuming the indentation transducer and cantilever under test could be treated as parallel linear springs attached to a mass, as shown in Fig. 1 so that

$$k_c = k_m - k_i \tag{2}$$

where k_c, k_m and k_i are the spring constants of the cantilever under test, the total system spring constant, and the indentation transducer spring constant, respectively. These values of k are determined by assuming the dynamic system could be treated as a lumped-mass harmonic oscillator in which

$$k = \frac{F}{Z}\cos\varphi + m\varpi^2 \tag{3}$$

where F is the amplitude of the sinusoidal force, Z is the amplitude of the resulting displacement, φ is the phase angle between the force and displacement, m is the mass of the system, and ω is frequency. A schematic of this experiment is shown in Fig. 1.

For the purposes of the indentation analysis, the effects of contact compliance and machine compliance were ignored. Although these compliances would add in series with the compliance of the cantilever, the compliance of the stiffest cantilever tested was on the order of 0.1 m/N. The contact compliance was measured to be approximately 2×10^{-4} m/N, and the machine compliance to be on the order of 10^{-7} m/N by indenting a silicon and fused quartz surface, respectively. These terms can both be safely discounted at the current level of uncertainty.

A Hysitron Triboscope instrumented indenter was used for all indentation measurements. The force measurements were calibrated against an auxiliary transducer that had in turn been calibrated with SI-traceable deadweights [19]. A cube-corner indenter tip was first lowered into contact with the surface of the cantilever under test, deflecting the cantilever and the internal spring of the indentation transducer until a contact force of approximately 2 μN was reached. A precision motion stage and proximal optical microscope allowed positioning of the indenter within a micrometer of the desired test location. This location was verified for the stiffer points near the base of the cantilever by using the indenter tip as a scanning probe to obtain topographical images of the fiducial marks.

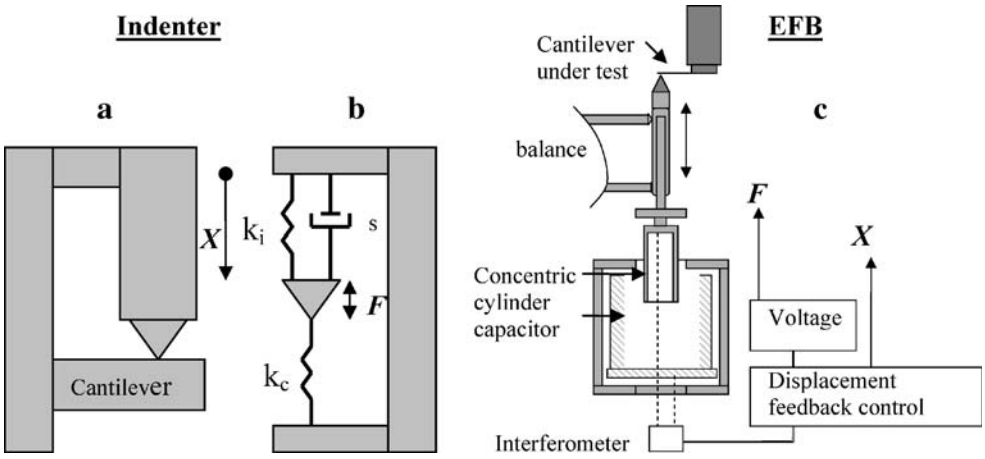

Fig. 1. Experimental schematics of the indentation and EFB methods for measuring k. (**a**) shows the indentation method, in which a sinusoidally varying force calibrated with deadweights is applied to the cantilever, and displacement is monitored with a lock-in amplifier. The *mechanical block diagram* of the system is shown in (**b**), and s is viscous damping of the system, which is small at the test frequency. (**c**) shows the EFB, displacement is measured interferometrically while a traceable electrostatic force is applied to maintain a null position

To determine k_m in equation (2) the force applied by the indentation transducer was then increased to 10 μN and a sinusoidal force of amplitude 7.5 μN at 10 Hz was added. This dynamic test allowed measurement of system spring constants using equation (3). It is important to note that both the bias and oscillating forces work against the combined stiffness of the indentation transducer (153 N/m) and reference cantilever, as is discussed in the uncertainty analysis below. This is in contrast to the preload, where a contact force of 2 μN is applied directly to the cantilever. The displacement amplitude was measured using the indentation transducer's integrated capacitive sensor in conjunction with a lock-in amplifier operating with a 10-s integration time [25, 26]. The spring constant of the indentation transducer, k_i, was determined by applying the bias and sinusoidal forces to the indenter while it was not in contact with the cantilever under test.

Thermal drift can be a large source of uncertainty in determining k using the indentation apparatus. The measurements were therefore performed in an environment where temperature was controlled to 0.02°C. The indenter was allowed to thermally equilibrate for at least several hours in this closed, vibrationally isolated environment before testing.

Electrostatic Force Balance

The NIST electrostatic force balance uses traceable measurements of distance (e.g., interferometry), capacitance, and voltage to realize an SI-traceable electrostatic force [27]. The central principle behind its operation is the use of a concentric cylinder capacitor, the inner electrode of which is connected to a movable balance arm. Because of the capacitor geometry, the capacitance, C, between the two electrodes is linear with position, Z, at the level of approximately 1 part in 10^4. This allows for the controlled application of a force according to

$$F = \frac{1}{2}\left(\frac{dC}{dZ}\right)V^2 \tag{4}$$

where V is voltage between the inner and outer electrodes. Because applied force and displacement are obtained traceably, this allows for a very direct determination of k. To this end, a spheroconical indenter tip was attached to the moving arm of the balance, and used to contact the cantilever under test. The position of this indenter tip with respect to the cantilever under test was controlled using a precision translation stage. A proximal microscope allowed placement of the indenter tip within 2 μm of the desired test point. Measurements were performed in vacuum while the position of the balance was controlled through a displacement of 2.5 μm while force was measured. A schematic of the experiment is shown in Fig. 1.

Transfer of Measurements to AFM

Once k is measured for individual points on the reference cantilever, it can be used to transfer the spring constant measurement to an AFM. Measurements were performed using a commercial AFM and a rectangular intermittent-contact imaging cantilever with nominal dimensions 160, 50, and 4.6 μm and a nominal spring constant of 42 N/m. The imaging cantilever was coarsely positioned using a micrometer stage and proximal optical microscope, and then a topographical image of the fiducial mark on the reference cantilever was obtained. This allowed very

precise definition of the point of contact between the reference and imaging cantilevers. The imaging cantilever was then pressed into the reference cantilever to a maximum deflection of approximately 100 nm to determine the spring constant of the combined system. This result was then compared to results obtained from the thermal method of determining k as implemented by the AFM manufacturer [11].

The configuration used to sense the cantilever deflection was the optical lever configuration typical in most AFMs. A laser beam reflected off the back of the cantilever is detected with a four-quadrant photodiode. The cantilever's deflection is detected as the reflected laser spot moves across the photodiode, causing a change in voltage between the upper and lower half of the detector. The AFM used in this experiment was equipped with a linear variable differential transformer (LVDT) displacement sensor that had been calibrated interferometrically by the vendor for the Z direction. By pressing the tip of the cantilever into a hard surface, the sensitivity of the quad-cell signal to cantilever deflection, δ, can be determined by comparing to the displacement measurement from the LVDT. For small displacements (approximately 100 nm in our case), the cantilever deflection is approximately linear. δ is then calculated using an automatic software routine provided by the vendor in which a linear least squares fit to the LVDT vs. detector voltage curve just after the cantilever contacts the surface is performed, as is shown in Fig. 2. The LVDT vs. detector voltage exhibited a slight hysteresis upon retracting the cantilever from the surface. Since it exhibited better linearity with displacement, the data from the cantilever approach was used when determining δ.

Once the AFM cantilever has been precisely positioned over the appropriate location, it is then pressed against the reference cantilever. The sensitivity of the quad-cell signal to the combined deflection of the AFM and reference cantilevers, δ_c, can be calculated using the same method as described above for determining δ. As long as the spring constant of the reference, k_{ref}, is well known, the spring constant of the imaging cantilever can then be determined from [15]

$$k_a = k_{ref}\left(\frac{\delta_c}{\delta} - 1\right)\sec\,\theta \tag{5}$$

where θ is the angle between the imaging cantilever and the surface. As a cross check to the cantilever on cantilever method, the thermal vibrational spectrum of the AFM cantilever was also used to determine k. The AFM manufacturer's software includes an algorithm which fits the power spectral density of the detector voltage to a single degree of freedom harmonic oscillator model. Using the parameters extracted from this fit and the measurement of δ, one can extract the spring constant of the cantilever using the equipartition theorem [11, 24].

Results

The values and associated uncertainties for k of the reference cantilever determined using the indenter and the EFB are summarized below in Table 1. In all cases,

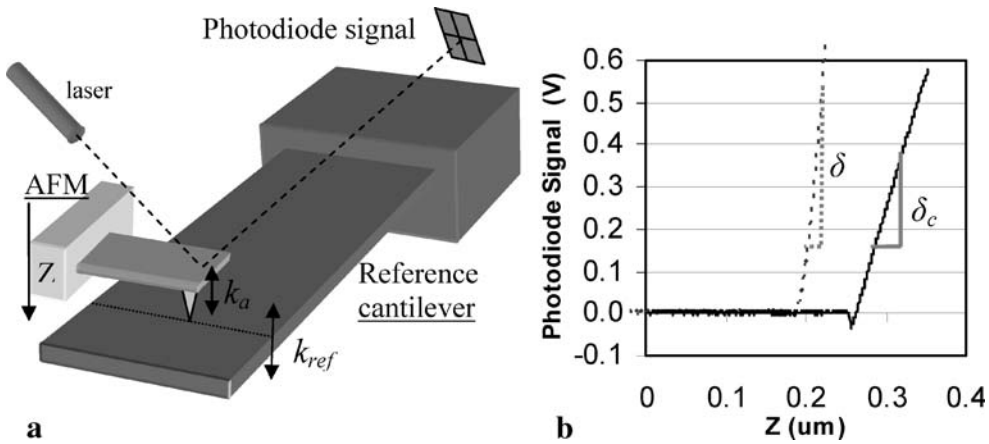

Fig. 2. (**a**) shows a schematic diagram of the cantilever-on-cantilever stiffness calibration method. The imaging cantilever is lowered into contact with the reference cantilever, and then the AFM is used to displace the imaging cantilever in the Z direction. As it does so, the imaging cantilever bends causing the reflected laser spot to move across the photodiode. (**b**) Shows data collected from this experiment. The *dashed line* is photodiode signal as a function of AFM displacement as the imaging cantilever is lowered into contact with a rigid surface. The *solid line* shows the same experiment in contact with the reference cantilever. The transient δ and δ_c can be calculated from these two curves and used in equation (5) to calculate the spring constant of the imaging cantilever, k_a, as long as the spring constant of the reference cantilever at the test point, k_{ref}, is accurately known

the two values agree within experimental uncertainty. For spring constants greater than 2 N/m, the results agree within 2%.

The values reported for the indentation method are the means of three trials conducted on different days. Each trial consisted of a determination of k for all of the points tested on the reference cantilever. Each determination represents the average of 100 measurements of k_m. The value of k_i was determined for the day by averaging 100 measurements, and assumed to be constant for each of the three points tested on the same day. The EFB measurements are the means of 25 determinations of the spring constant at each point tested on the reference cantilever.

Test point 1 of the reference cantilever was used to calibrate an imaging cantilever with an AFM as described above. A thermal method was also used to calibrate the imaging cantilever. This thermal cross-check included a first-order correction for laser spot size and location along the length of the cantilever, under the assumption that a very small laser spot was positioned at the end of the imaging cantilever [12]. The spring constant determined using the reference cantilever agreed with that determined by the thermal method within experimental uncertainty, as is shown in Table 2.

Discussion of Uncertainty

Overnight equilibration in a controlled environment allows for a standard deviation of 0.044 N/m in the determination of k_m. However, a standard deviation of 0.062 N/m is also present during the determination of k_i which is necessary to determine k from equation (2). These type A uncertainties were determined by calculating the standard deviation of each set of 100 data points used to measure k_m and k_i, and then determining the mean value of this standard deviation over the course of the three trials conducted. Using the root-sum-of-squares (RSS) method [21], this results in a combined type A uncertainty of 0.076 N/m. This statistical uncertainty is inherent in the measurement system, and remained approximately the same for all spring constants tested.

Table 1 Measured cantilever spring constants and their uncertainties

Test point	k_c indentation (N/m)	k_c EFB (N/m)
1	18.90 ± 0.76	18.883 ± 0.659
2	2.03 ± 0.09	2.0656 ± 0.031
3	0.40 ± 0.08	0.461 ± 0.004

Table 2 Comparison of reference cantilever and thermal methods

k_a AFM	k thermal
55.7 ± 3.3 N/m	53.8 ± 2.1 N/m

It should be noted that the type A uncertainty may be convoluted with the effects of a small amount of mechanical drift in the system.

To determine k from equation (3), the force and displacement measurements must be accurately calibrated. The force measurements have been calibrated using an auxiliary capacitive sensor and deadweights, as described in a previous study [19]. This allows measurement of force with an uncertainty of 1%. Displacement sensitivity of the indentation transducer was calibrated by the vendor using an interferometer. Checking the spring constant specified by the vendor against the value of k_i determined from the dynamic test results gives agreement within 1% at 10 Hz. This indicates consistency with the vendors' interferometry. Both of these are systematic, and are uncertainties determined by non-statistical methods (i.e., type B uncertainties). As above, these uncertainties must be counted twice when calculating combined standard uncertainty because they are present when measuring both k_m and k_i for use in equation (2). They are summed using the RSS method as described above to determine type B uncertainty due to displacement and force measurement in Table 3.

Deviations from the linear Hooke's law behavior assumed in this analysis may be present if the cantilever is deflected too far. Nonlinearity may arise

Table 3 Sources of uncertainty for the dynamic indentation results presented in Table 1

Source of uncertainty	Magnitude of uncertainty
Statistical uncertainty	0.076 N/m
Displacement measurement	0.01 k
Force measurement	0.01 k
Position of indenter on cantilever under test	$u_p = 3\left(\frac{\Delta L}{L_i}\right)k$
Combined Standard Uncertainty	$\left[0.076^2 + 4(0.01\,k)^2 + u_p^2\right]^{1/2}$

Terms in which k is included reflect that these relative uncertainties dependent on the value of the spring constant. Combined standard uncertainty is calculated as the root sum of squares of the individual components, and is dependent on the test point, as is reflected in equation (7). Recall that equation (2) requires two spring constants to be experimentally determined, so the uncertainties in both force and displacement are counted twice in the combined standard uncertainty.

from the indentation transducer and from the reference cantilever itself at large enough displacements. During the calibration, oscillating and bias forces of 7.5 μN and 10 μN, respectively, were applied against the combined stiffness of the cantilever, and the internal spring of the indentation sensor which has stiffness of k_i = 153 N/m. The total stiffness of the system is $k_c + k_i$, which ranges from 154 to 173 N/m. This results in DC displacements around 60 nm, and AC displacements of amplitude around 40 nm peak-to-peak in the combined cantilever/transducer system.

The deflections were well within their linear regimes of the cantilevers tested in all cases.

For an Euler–Bernoulli beam (e.g., bending moment is proportional to curvature), it is typical to write

$$M = EI\frac{\partial^2 y}{\partial x^2} \tag{6}$$

where M is bending moment, x is a coordinate along the cantilever length and y is a coordinate normal to its length. However, this is a linear approximation to

$$M = \frac{EI\frac{d^2y}{dx^2}}{\left[1+\left(\frac{dy}{dx}\right)^2\right]^{3/2}} \tag{7}$$

Expanding equation (7) for small values of the slope, dy/dx, we have

$$M = EI\frac{d^2y}{dx^2}\left[1-\frac{3}{2}\left(\frac{dy}{dx}\right)^2+\ldots\right]. \tag{8}$$

Thus, to obtain the linear approximation, deflection should be limited such that $dy/dx < 0.08$, confining nonlinearities in moment to the sub-percent level. The relation between displacement and slope for a cantilever beam subject to point loadings at a position along its length is

$$\frac{dy}{dx} = \frac{3z}{2L} \tag{9}$$

where z is displacement. At test point 3 on the reference cantilever, for example, l = 712 μm, so displacement should be kept below 38 μm. The 2 μN contact force used as a preload deflects the cantilever approximately 5 μm at this test point, which clearly satisfies this condition.

The other terms in equation (3) contribute much less to the uncertainty. The phase angle (φ) is part of a cosine term, and its value was measured to be less than 0.1° in all experiments. It contributes a maximum systematic uncertainty of 2×10^{-6} of the value of k, and is therefore not explicitly included in the combined standard uncertainty.

The inertia term in equation (3) ($m\omega^2$) is also a minor contributor to uncertainty. Estimating the mass of the cantilever under test using the approximate dimensions and the density of single crystal silicon (2,990 kg/m^3) yields approximately 10^{-3} mg. Therefore the increase in system mass upon contacting the cantilever beam is negligible. Furthermore, the vendor of the lock-in amplifier specifies the standard type B uncertainty in frequency to be 3×10^{-6} Hz, which means frequency is constant at this level whether the indenter is in contact with the cantilever or not. Therefore the inertia term [$m\omega^2$ in equation (3)] can be eliminated as a common mode term in equation (2), resulting in a type B, systematic uncertainty of approximately 3×10^{-6} N/m. Since this uncertainty is less than 1 part in 10^4 of the total uncertainty, it is not explicitly included in the combined standard uncertainty analysis at this time.

The accuracy of the spring constant determination hinges upon locating the point of contact between the indenter and cantilever under test. This is greatly aided by the presence of microfabricated fiducial marks on the cantilever, which specify test points. An optical microscope allowed for placement of the indenter tip within 2 μm of the desired test location using an encoded three-axis translation stage. The stiffness remained constant within experimental uncertainty as long as the point of contact remained within several micrometers from the center of the cantilever transverse to its longitudinal direction. Since the instrumented indenter is capable of operation as a scanning probe microscope, the indenter tip was used to scan the fiducial marks, and verify placement within 2 μm of the desired test point. Therefore, assuming Euler–Bernoulli beam theory holds as in equation (1), the type B uncertainty in k due to placement of the indenter tip can be estimated as

$$u_p = 3\left(\frac{\Delta L}{L_t}\right)k \tag{10}$$

where ΔL is the uncertainty in tip placement (2 μm), and L_t is the distance from the base of the cantilever to

Table 4 Sources of uncertainty the in EFB results from Table 1

Source of uncertainty	Magnitude of uncertainty
Displacement measurement	$0.002\,k$
Force measurement	$10^{-4}\,k$
Position of indenter on cantilever under test	$u_p = 3\left(\frac{\Delta L}{L_t}\right)k$
Combined Standard Uncertainty	$\left[(0.002\,k)^2 + (10^{-5}k)^2 + u_p^2\right]^{1/2}$

the test point. The values of l_t are 172, 412, and 712 μm for test points 1, 2, and 3, respectively.

The sources of uncertainty, their magnitudes, and the combined standard uncertainty [21] of the dynamic indentation results shown in Table 1 are summarized in Table 3. It should be noted that these uncertainties apply to a reference cantilever which is intended to be used to transfer the spring constant to an AFM cantilever as described below. If the spring constant measurement is to be performed directly on the AFM cantilever, care must be taken to measure k at the sharp tip of the AFM cantilever, or indent a flat area near the AFM cantilever tip and add an additional position uncertainty as in equation (10).

In the EFB, a traceable electrostatic force is realized directly through measurements of SI electrical quantities with uncertainties on the order of 1 part in 10^4 [i.e., the uncertainty of the capacitance gradient in equation (4)]. Likewise, displacement is measured interferometrically with 1-nm uncertainty. Once again, the uncertainty of the spring constant measurement was limited by the accuracy in placement of the indenter tip, yielding a type B uncertainty as per equation (10). The machine compliance of the balance was measured to be approximately 2×10^{-4} m/N, and was not included in the analysis. The uncertainties associated with the EFB measurements are listed in Table 4.

When the SI-traceable cantilever calibration was transferred to an AFM, the effect of uncertainty in the location of the point of contact was greatly reduced. The AFM allowed the desired test point to be located within a few tens of nanometers by using its topographical imaging capability. The transfer of k in this case was primarily limited by the problems inherent in using a cantilever beam as a force sensor. The AFM cantilever is itself a passive force sensor, meaning that its ability to measure force stems from the measurement of its deflection in response to that force. As the cantilever bends in response to an applied force, there is relative motion between the tip and surface. For the 100-nm deflections used, the relative motion is approximately 20 nm. This leads to the off-axis forces arising from friction between the cantilever tip and the surface which may not be constant for different substrates. It should be noted that these effects are present in both the reference cantilever and thermal methods, as both require pressing the cantilever against a hard surface to calibrate the photodiode sensitivity to cantilever deflection. As such, only type A uncertainty determined from the standard deviation of five trials is quoted in Table 4. These results highlight the fact that the uncertainties in AFM force measurement are application specific, often depending on the properties of the surfaces being examined. Further work will be necessary to exactly quantify and minimize uncertainty due to contact mechanics. However, their contribution to experimental uncertainty can be minimized by performing a true non-contact calibration, or by compensating for the relative motion using the scanning stage of the AFM [4, 22].

Conclusion

Methodology has been outlined for SI-traceable determination of microfabricated cantilever spring constants, and a dynamic force indentation method was compared against the NIST EFB. Both methods involve using a physical contact between an instrument which measures force and displacement directly, and in both cases, uncertainty is limited by accurate placement of the probe. Agreement within experimental uncertainty has been demonstrated, as well as absolute agreement within 2% for spring constants greater than 2 N/m. Transferring the calibrated beam to an AFM allows for cantilever on cantilever spring constant calibration which agrees with the thermal method within 5%. The use of a reference cantilever as a transfer artifact will allow the use of AFM to perform SI-traceable small force measurement provided the reference cantilever can be calibrated accurately.

Acknowledgments The authors wish to thank Dr. Richard Seugling for assistance in force calibration of the instrumented indentation apparatus, and Dr. Peter Cumpson for providing the reference cantilever. Gordon Shaw was supported by a National Research Council NIST postdoctoral fellowship.

References

1. Dixson R, Guerry A (2004) Reference metrology using a next-generation CD-AFM. Proc. SPIE, 5375, pp 633–646.
2. Smith SB, Cui Y, Bustamante C (1996) Overstretching B-DNA. Science 271:795–799.
3. Rief M, Gautel M, Oesterhelt F, Fernandez JM, Gaub HE (1997) Reversible unfolding of individual titin immunoglobulin domains by AFM. Science 276:1109–1112.
4. VanLandingham MR (2003) Review of instrumented indentation. J Res Natl Inst Stand Technol 108:249–265.
5. Rugar D, Budakian R, Mamin HJ, Chui BW (2004) Single spin detection by magnetic resonance force microscopy. Nature 430:329–332.
6. Poogi MA, McFarland AW, Colton JS, Bottomley LA (2005) A method for calculating the spring constant of atomic force microscopy cantilevers with a nonrectangular cross-section. Anal Chem 77:1192–1195.
7. Sader JE (1995) Parallel beam approximation for V-shaped atomic force microscope cantilevers. Rev Sci Instrum 66: 4583–4587.

8. Blank K, Mai T, Gilbert I, Schiffmann S, Rankl J, Zivin R, Tackney C, Nicolaus T, Spinnler K, Oesterhelt F, Benoit M, Clausen-Schaumann H, Gaub HE (2003) A force-based protein biochip. PNAS 100:11356–11360.
9. Cleveland JP, Manne S, Bocek D, Hansma PK (1993) A nondestructive method for determining the spring constant of cantilevers for scanning force microscopy. Rev Sci Instrum 64:403–405.
10. Sader JE, Pacifico J, Green CP, Mulvaney P (2005) General scaling law for stiffness measurement of small bodies with applications to the atomic force microscope. J Appl Phys 97:124903–124907.
11. Hutter JL, Bechhoefer J (1993) Calibration of atomic force microscope tips. Rev Sci Instrum 64:1868–1873.
12. Proksch R, Schaffer TE, Cleveland JP, Callahan rC, Viani MB (2004) Finite optical spot size and position corrections in thermal spring constant calibration. Nanotechnology 15:1344–1350.
13. Senden TJ, Ducker WA (1994) Experimental determination of spring constants in atomic force microscopy. Langmuir 10:1003–1004.
14. Vladar A, Villarrubia JS, Postek MT (2003) A new way of handling dimensional measurement results for integrated circuit technology. Proc. SPIE, 5038, pp 508–517.
15. Cumpson PJ, Clifford CA, Hedley J (2004) Quantitative analytical atomic force microscopy: a cantilever reference device for easy and accurate AFM spring-constant calibration. Meas Sci Technol 15:1337–1346.
16. Torii A, Sasaki M, Hane K, Okuma S (1996) A method for determining the spring constant of cantilevers for atomic force microscopy. Meas Sci Technol 7:179–184.
17. Scholl D, Everson MP, Jaklevic RC (1994) In situ force calibration of high force constant atomic force microscope cantilevers. Rev Sci Instrum 65:2255–2257.
18. Holbery JD, Eden VL, Sarikaya M, Fisher RM (2000) Experimental determination of scanning probe microscope cantilever spring constants utilizing a nanoindentation apparatus. Rev Sci Instrum 71:3769–3776.
19. Seugling RA, Pratt, JR (2004) Traceable force metrology for micronewton level calibration. Proc. ASPE, Annual Meeting, Orlando, FL.
20. Pratt JR, Smith DT, Newell DB, Kramar JA, Whitenton E (2004) Progress toward Systeme International d'Unites traceable force metrology for nanomechanics. J Mater Res 19:366–379.
21. Taylor BN, Kuyatt CC (1994) Guidelines for evaluating and expressing the uncertainty of NIST measurement results. NIST Technical Note 1297.
22. Cannara RJ, Brukman MJ, Carpick RW (2005) Cantileer tilt compensation for variable-load atomic force microscopy. Rev Sci Instrum 76:537061–537066.
23. Cumpson PJ, Hedley J (2003) Accurate analytical measurements in the atomic force microscope: a microfabricated spring constant standard potentially traceable to the SI. Nanotechnology 14:1279–1288.
24. Proksch R, Cleveland J (2005) Quantifying molecular forces: sensitivities and spring constants without touching a surface. Asylum Research Technical Note.
25. Dynamic stiffness measurement. Hysitron, Applications Note.
26. Syed Asif SA, Wahl KJ, Colton RJ (1999) Nanoindentation and contact stiffness measurement using force modulation with a capacitive load-displacement transducer. Rev Sci Instrum 70:2408–2413.
27. Pratt JR, Kramar JA, Newell DB, Smith DT (2005) Review of SI traceable force metrology for instrumented indentation and atomic force microscopy. Meas Sci Tech 16: 2129–2137.
28. Holbery JD, Eden VL (2005) A comparison of scanning microscopy cantilever force constants determined using a nanoindentation testing apparatus. J Micromechanics Microengineering 10:85–92.